PARAMETRIC INVESTIGATION OF A DIELECTRIC BARRIER DISCHARGE PLASMA ACTUATOR

A Paper
Submitted to the Graduate Faculty
of the
North Dakota State University
of Agriculture and Applied Science

By

Narender Goud Bejawada

In Partial Fulfillment of the Requirements
for the Degree of
MASTER OF SCIENCE

Major Department:
Mechanical Engineering and Applied Mechanics

March 2010

Fargo, North Dakota

North Dakota State University
Graduate School

Title

Parametric Investigation of a

Dielectric Barrier Discharge Plasma Actuator

By

Narender G. Bejawada

The Supervisory Committee certifies that this ***disquisition*** complies with North Dakota State University's regulations and meets the accepted standards for the degree of

MASTER OF SCIENCE

ABSTRACT

Bejawada, Narender Goud, M.S., Department of Mechanical Engineering and Applied Mechanics, College of Engineering and Architecture, North Dakota State University, March 2010. Parametric Investigation of a Dielectric Barrier Dishcarge Plasma Actuator. Major Professor: Dr. Zakaria Mahmud.

The dielectric barrier discharge (DBD) plasma actuator is considered an effective flow control device in various aerospace applications such as drag control, lift control, and stall control. The DBD plasma actuator has many potential benefits in active flow control applications, such as an absence of moving parts and low power draw. Numerous studies have been done to estimate the effect of plasma flow on specific aerospace applications. These studies have revealed that the performance of the plasma actuator depends on a number of parameters, such as operating voltage and currents, materials, and the surrounding air velocity, to name a few. Unique combinations of these parameters are required for optimal performance of the actuator; therefore, robust parametric studies have been undertaken to fully predict the plasma-based flow fields. The present study focuses on evaluating the influence of electrical, geometrical and material parameters on the single DBD plasma actuator flow. The electrical parameters include voltage and frequency, whereas electrode gap orientations and dielectric materials are considered geometrical and materials parameters, respectively. The parametric study was done by estimating the plasma-induced velocity in quiescent media with the Particle Image Velocimetry (PIV) system for various actuator settings and operating conditions. The effects of the above parameters and characteristic behavior on the single DBD plasma actuator are discussed and compared. The obtained maximum velocities for different settings and operating conditions are used as a basis for comparison. Results showed that the operating voltage

was the major parameter influencing the actuator performance, and the electrode gap orientations (±1 mm) had negligible effect.

ACKNOWLEDGEMENTS

I would like to convey my sincere thanks to my advisor, Dr. Zakaria Mahmud, for providing me a wonderful opportunity to work with him and for his patience. He has been very supportive throughout this work, and his knowledge has been a great privilege for me. I would like to thank NASA EPSCoR for their financial support. I would also like to thank my graduate committee members, Dr. Alan Kallmeyer, Dr. Majura Selekwa and Dr. Subbaraya Yuvarajan for being my committee members and spending their valuable time reviewing my paper despite their busy schedules.

The moral support of my family, friends and colleagues throughout this work added a great value to it, and I would like to convey my special thanks to all.

TABLE OF CONTENTS

LIST OF TABLES

LIST OF FIGURES

CHAPTER 1. INTRODUCTION

In the past ten years, study of the DBD (dielectric barrier discharge) plasma flow has received attention because of its variety of applications. DBD plasma flow is mainly used in aerospace applications or flow control applications, and it is also used in material processing and noise control applications such as landing gear noise reduction. The flow control applications include drag reduction, lift control, and stall control. Previously, practiced traditional flow control techniques for these applications were the creation of suction or blowing on the surface, the addition of roughness to the surface and surface vibration. DBD plasma flow was proven more effective and preferable to these applications when compared to traditional flow control methods, as it has some advantages over the traditional flow control methods such as low cost, no moving parts, low weight, reliability and easy assembly.

The present paper focused on a single DBD plasma actuator, which consists of two electrodes that are asymmetrically separated by a dielectric material and which is shown in Figure 1.1 (a).

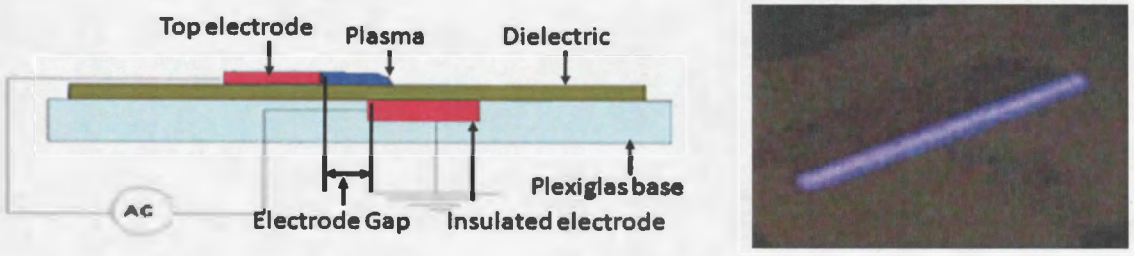

(a) (b)

Figure 1.1. Single dielectric barrier discharge actuator.

The top electrode is exposed to the atmosphere, whereas the bottom electrode is covered by the dielectric material. On applying an A.C. voltage across these electrodes, plasma discharge is produced on the dielectric surface. The photograph (see Figure 1.1 (b)) was taken when the actuator was operating at certain conditions. The electrodes used in the actuator are mostly made of highly conductive materials (copper and steel, for example), and materials with higher dielectric strengths are chosen for the dielectric material (Kapton, and Teflon, for example.). Depending on the applications, actuators can be constructed in various shapes and sizes, such as rectangular or circular. Circular actuators are often used to create synthetic jets[1-6].

The mechanism behind the plasma discharge production in the single DBD plasma actuator has been well explained by previous authors[7-11]. The plasma discharge occurs when an electric field with sufficient voltage and frequency is supplied to the SDBD actuator and that field is surrounded by a small volume of gas. The electrons from the electric field collide with the surrounding neutral gas and these collisions result in ionization of the gas (also called plasma discharge). Enole et. al[7-11] explained that the produced plasma in both half cycles in A.C. voltage was not the same. On applying an A.C. voltage to the actuator, in the negative half cycle, the cathode emits electrons to reach the bottom electrode. These electrons are stopped by the dielectric material, and are then bombarded with the surrounding neutral air, resulting in ionization as shown in Figure 1.2 (a). In Figure 1.2 (b), for the positive half cycle (opposite half cycle), the discharge that is deposited on the dielectric surface behaves as a cathode and tends to move toward the exposed electrode. In the negative half cycle (see Figure 1.2 (a)), the discharge is uniform

and continuous, and in the positive half cycle, the discharge is non-uniform and discontinuous (see Figure 1.2 (b)).

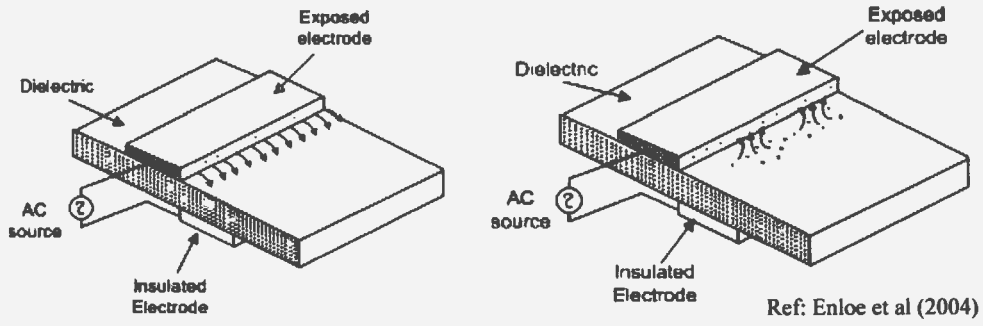

(a) Negative going half cycle (b) Positive going half cycle

Figure 1.2. Behavior of the plasma discharge in both cycles.

The plasma discharge provides momentum or velocity to the surrounding medium in the direction of the plasma flow. This phenomenon is clearly shown in Figure 1.3; here the flow surrounded by the actuator is being drawn toward the tip of the actuator and then pushed downstream with a velocity. This induced velocity into the flow field was varied from zero to maximum value and was based on the obtained maximum velocity for which the performance of the plasma actuator was estimated. This performance or maximum

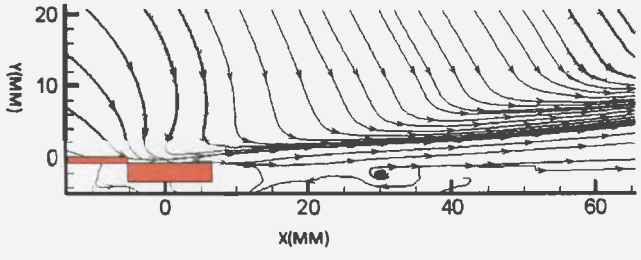

Figure 1.3. Effect of the plasma flow on the flow field.

velocity may vary with a variation in the parameters. Various studies have been done to estimate the parameters' effects on the performance of the DBD plasma[11-17]. The parameters that affect the plasma performance are electrical (voltage, frequency, waveform), geometrical (electrode gap, shape and size of electrode/dielectric, electrode orientation) and material (dielectric/electrode). With regard to electrical parameters (voltage, frequency and waveform), it has been documented that an increase in voltage will increase the velocity, as the electric field surrounding the exposed electrode increases as well. This increase results in higher Colombian forces between the ions and pushes the surrounding gas with a higher velocity in the surrounding medium[11]. The increase in frequency also increases the velocity, as the increase in frequency speeds up the rate of bombardments or collisions between ions and electrons, and that increase results in high strength plasma with higher induced velocity[11]. Previous studies have shown that the typical voltage and frequency ranges used in plasma actuators were about 4 kV to 30 kV and about 200 Hz to 10 kHz, respectively. The wave effect was not considered for most of the studies and the most common A.C. waveform used in these actuators was the sine wave.

With regard to geometrical parameters, the electrode gap significantly affects the overall performance of the plasma actuator. An increase in the electrode gap will increase the velocity as the plasma discharge expansion length increases. Earlier research has shown that the positive gap (about 1 mm to 5 mm) between the electrodes resulted in higher performance (higher induced velocity) when compared to the negative gap (overlap) or no gap configurations[11,12,15]. The range considered for the electrode gap study was from

(-5 mm to 15 mm) [11,12,15]. Figure 1.4 shows the electrodes with various gaps and their nomenclatures.

Figure 1.4. Different electrode gap orientations.

Unlike electrode gap orientations, the electrode sizes and shapes have little or no effect on plasma strength. The plasma performance also varies with the thickness of the dielectric material (typically 1 mm to 3 mm). As the thickness of the dielectric material decreases, the permittivity of the material increases, thus the performance of the actuator increases. However, using the thinnest material will result in filamentary instabilities, which results in dielectric material failure even at lower voltages [11].

The materials with higher conductivity are generally used for electrodes and there weren't sufficient studies done on electrode material effects. Aluminum, tungsten, steel and copper are some common materials for electrodes, with copper the most common choice. Permittivity and the dielectric strength are two major characteristics of the dielectric materials affecting the plasma performance. The permittivity of the material increases the plasma-induced velocity, which is due to the increase in the electric field. The higher dielectric strength helps to operate at higher voltages and frequencies. The most common and widely used dielectric material is Kapton. However, Alumina ceramic, Teflon, quartz, mica, glass, and PMMA, to name a few, were also used in previous studies[11,12]. In a study

of the impact of dielectric materials on the plasma actuator, Teflon and quartz have shown better performance with higher velocity[12].

More investigations are needed for a better understanding of DBD plasma characteristics, as few studies have been done. While studying the influence of the supplied voltage and frequency, most studies dealt with high voltage ranges (for example, greater than 20 kV) with low frequencies (for example, less than 2 kHz) or moderate voltage ranges (4 kV to 10 kV) with high frequencies (4 kHz to 10 kHz). There were very few studies on low voltage ranges (less than 4 kV) at higher frequencies (5 kHz to 15 kHz). Among the geometrical parameters, the electrode gap has been one of the most highly examined. While studying the influence of the electrode gap, previous researchers often used higher gap increments (~2.5 mm up to 5 mm steps), and although some of them used lower gap increments (1 mm), they did not study the plasma behavior when electrodes are overlapped by 1 mm; therefore, it is important to understand the physics at lower gap increments with 1 mm overlap (~1 mm steps). There were very few studies using Alumina ceramic as the dielectric material.

The objective of the present work was to characterize a DBD plasma actuator to obtain effective performance and also to estimate the effect of parameters such as voltage, frequency, electrode gap and material on the induced velocity. The study focused on the lower voltage range (2.8 kV to 4.2 kV) at a higher frequency (5 kHz to 15 kHz). The sine waveform was used for this study. The research also focused on the electrode gap effects with small increments (1 mm steps) from -1 mm overlap to 1 mm gap, and the dielectric material effect was estimated using Kapton and Alumina ceramic. The effects of the waveform, thickness, size and shape of the electrodes were not studied.

CHAPTER 2. LITERATURE REVIEW

Due to the numerous applications of the DBD plasma, it has been studied both experimentally and numerically[1-22]. These studies involved the direct measurement of the force, the induced velocity and the power consumption of the actuators at varying operating, geometric and material parameters. The performance of the plasma actuators depended on the following parameters: the supplied voltage, frequency, cycle waveform or power waveform, electrode and dielectric geometries, electrode orientation, materials, ambient pressure, free stream velocity, and surrounding medium (gases). For flow control applications, the performance of the plasma actuator was judged by the induced velocity (or momentum) production. Thus, to optimize the strength of the actuators, previous researchers compared the velocity production at varying parametric combinations. Some studies compared the thrust production to optimize the performance[13,14].

2.1. Electrical parameters

The applied voltage effect on different dielectric barrier actuators showed that the velocity increased with an increase in voltage at constant frequency. The voltage range examined was from 4 kV to 30 kV [11,12,13]. Most of these variations followed the parabolic trend. However, Roth et al. [12] observed that the induced velocity peaked between 7 kV and 8 kV when they varied the voltage from 4 kV to 10 kV at different constant frequencies (from 5 kHz to 10 kHz) as shown in Figure 2.1 (a). Abe et al.[13] showed that the velocity increased linearly with an increase in voltage for the range of 4.2 to 7.7 kV at a frequency of 5 kHz. There was a study performed on two different voltages, such as 10 kV and 20 kV

at a frequency of 300 Hz, and the results showed the velocity to be higher at the higher voltage of 20 kV[15].

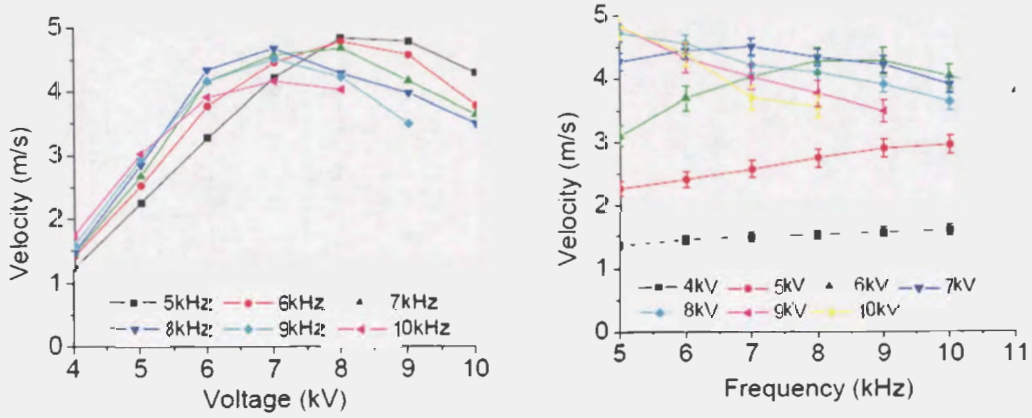

a) Plasma induced velocity with frequency increment at different voltages

b) Plasma induced velocity with voltage increment at different frequencies

Ref: Roth et al.

Figure 2.1. Plasma induced velocity with frequency and voltage increment.

Previous studies on the influence of frequency on the single DBD plasma actuators found that the velocity increased with an increase in frequency. The frequency range tested was from 200 Hz to 10 kHz at a constant voltage[11- 13]. Forte et al.[11] observed that the frequency peaked at 1.2 kHz and maintained almost the same value even though the frequency increased from 1.2 kHz to 2 kHz at a constant voltage of 20 kV. Van Dyken et al.[14] made similar observations as they varied the frequency from 3 kHz to 10 kHz with a peak velocity at 5 kHz. However, Roth et al.[12] varied the frequency from 4 kHz to 10 kHz at different constant voltages (from 4 to 10 kV), shown in Figure 2.1 (b). They observed that for voltages from 8 kV to 10 kV, the velocity peaked at lower frequencies such as 5

kHz. Previous results show that the frequency effect on the plasma-induced velocity was less when compared to the voltage, and that is shown in Figure 2.1.

The effects of frequency and voltage on velocity completely depend on each other. In previous studies[12], it was observed that at a high frequency such as 10 kHz, the velocity decreased as the voltage increased from 5kV to 10 kV. At a constant voltage of 10 kV, the velocity decreased as the frequency increased from 4 kHz to 10 kHz, because at higher voltages and frequencies, the discharge had no time to relax and was not able to capture all the electrons and ions that were produced. The discharge polarized, which resulted in filamentary instabilities and caused a decrease in velocity[11,12].

The power waveform studies were done with different waveforms, including the sine wave, the square wave with different duty cycles, and the triangular waveform (also called the saw toothed waveform). The most widely used waveform was the sine wave[8-10,11,13]. There were several studies on different waveforms, such as the saw tooth (also called the triangular waveform) and square waveforms[13,14,16]. The square waveform with different duty cycles was mostly used in high-speed flow applications. Balcon et al.[16] made an interesting observation about saw toothed waveforms. The negative saw tooth waveform produced higher velocities when compared to the positive saw tooth waveform. Van Dyken et al.[14] made different observations. The positive saw tooth waveform produced a higher thrust force when compared to other waveforms. Abe et al.[13] studied the slope of the waveform, and they considered the sine wave, positive saw-toothed and negative saw-toothed waveforms. They found that as the slope increased, the net momentum transfer increased. Previous observations indicated that there were very few parametric studies on the waveform effect.

2.2. Geometrical parameters

In relation to geometrical parameters, the electrode gap effect was studied by many researchers[11,12,15,18]. This type of study showed that the positive gap gave better results when compared to the negative gap cases[11,12,15,18]. Forte et al.[11] found the maximum velocity at a 5 mm gap for different dielectric barrier discharge actuators with a gap variation from -5 mm to 15 mm. The reason for obtaining more velocity at positive gaps was that, as the gap increased, the electrons had a chance to move forward, which, in turn, resulted in attaining more velocity. But after crossing a certain gap (for example, a 5 mm gap), velocity started to decrease as the net dielectric thickness increased. If they were overlapped, then there was less of a chance for ions to move down, and that resulted in less velocity [11,12]. Roth et al.[12] observed a different pattern as they varied the gap from 0 to 3 mm; the maximum induced velocity occurred at the 2 mm gap.

The electrode width is another geometric parameter that affects the plasma-induced velocity. Previous studies have found that a larger width of the ground electrode increased the induced velocity, because the plasma expanded more at a higher ground electrode width. This effect is noticed for widths up to 15 mm[11,12]. Forte et al.[11] varied the ground electrode width from 1 to 50 mm and observed that the induced velocity decreased at higher electrode widths (more than 15 mm). Dyken et al.[14] confirmed the observation of increasing velocity at increasing widths, while Roth et al.[12] reported a very small increase in the velocity with decreasing electrode widths.

Studies on dielectric layer thickness were also done and it was observed that the velocity decreased with an increase in thickness[11]. As the thickness decreased, the permittivity of the material increased. This resulted in a higher induced velocity and also

led to filamentary instability, which in turn led to dielectric failure. Forte et al.[11] noted higher velocities for 1 mm thick PMMA dielectric material, but it failed at 17 kV. The 2 mm thickness resulted in a higher velocity when compared to 3 mm up to 30 kV in the 1 to 3 mm thickness range.

There were also studies done on electrode orientations. Gibson et al.[17] investigated the effect of electrode arrangement. They arranged these materials in configurations such as Z type (electrodes are parallel to each other) and T type (electrodes are perpendicular to each other) and tested the arrangements at a voltage of 20 kV and a frequency of 700 Hz. The Z type actuator gave better performance by inducing more velocity parallel to the actuator surface when compared to the T type actuator, as the T type produced filamentary plasma normal to the surface and the distance travelled on the surface was less.

Overall, the affect of geometrical parameters on the plasma performance is less when compared to the electrical parameters, especially the voltage effect[11,12]. Studies showed that with regard to geometrical parameters, the parameter with the most influence on the plasma performance (plasma-induced velocity) was the gap between the electrodes.

2.3. Material parameters

The properties of the dielectric materials, such as permittivity and dielectric strength, were the key factors that influenced the behavior of the plasma actuators. As the permittivity of the material increased, the electric field also increased, which resulted in a higher velocity. This phenomenon has proven to be true at lower voltages[11,12], but at higher voltages the velocity starts decreasing for higher permittivity material because of higher dielectric loss factor[11,12]. The impact of dielectric permittivity totally depended upon the

operating voltage and frequency. Higher dielectric strength helped to operate thinner materials at higher voltages without any dielectric failure. For example, Kapton has a higher dielectric strength when compared to other materials, but it also has a higher dielectric loss factor when compared to other dielectric materials. Roth et al.[12] studied dielectric heating losses in detail, and concluded that quartz and Teflon are the best dielectric materials with a low dielectric loss factor. They tested quartz (permittivity (ε_r) = 5, Dielectric strength = 25 kV/mm) and Teflon (permittivity (ε_r) = 2.1, Dielectric strength = 11.2 kV/mm) actuators and found that the quartz actuator produced the highest velocity when compared to a Teflon actuator, but the Teflon actuator produced the highest velocity for a given power input. The reason was that at lower voltages (such as 4 kV and 5 kV), actuator materials with a higher permittivity material produced high velocity but also consumed more power; therefore, quartz actuators produced more velocity but also consumed more power, as the permittivity of quartz is higher than that of Teflon. Previous studies have shown that the effect of material parameters was less significant when compared with the electrical and geometrical parameters[11,12].

2.4. Other parameters

Various studies were done on multiple actuators, and it was observed that the use of multiple actuators improved the velocity induced by the plasma when arranged parallel to each other[2,3,14,15]. This was because the initial velocity value for the second actuator was not zero, which resulted in a higher induced velocity.

CHAPTER 3. EXPERIMENTAL SETUP AND PROCEDURE

Experiments were conducted in Dolve 131, the Fluid Mechanics Lab in the Mechanical Engineering Department, at North Dakota State University, Fargo, ND. The experimental facility, experimental arrangements and measurements are discussed in this chapter.

3.1. Experimental Facility

The experimental facility used for these experiments consisted of an A.C. power source, voltage and current probes and the particle image velocimetry (PIV) system.

A.C. power source

The A.C. power source consisted of a BK Precision 4017A 10 MHz Sweep function generator (viz., 20 V p-p open circuit a d 10V p-p into 50 Ω), PLX1802 Professional 1000 Watt audio amplifier (viz., input sensitivity: 1.28 Vr.m.s, frequency range: 20 Hz to 20 kHz and gain: 1: 20) and an Industrial CMI-6488 step-up transformer (viz., turns ratio: 1:137.5, input sensitivity: 80Vr.m.s and frequency limit: 20 kHz). This A.C. power source was capable of providing a voltage up to 20 kV at a frequency of 20 kHz.

Measuring devices

To measure the voltage and current of the plasma actuator, a PMK GMbh manufactured voltage probe (model PHV 4002-3 with x1000 Attenuation, 100 MHz, and 40kV peak pulse) and a Pearson current monitor (model 4100, sensitivity 1 volts/amp, max 5 amp rms) were used. The collected voltage and current data were transferred to the

computer with the help of the LABVIEW (version 8.2) program and digital oscilloscope (model TDS 2012B 1 Giga Samples/sec; 2500 points record length).

PIV

To map the velocity of the plasma-induced flow, the TSI model 2D Particle Image Velocimetry (PIV) system was used. The PIV system was equipped with a 532 nm Nd:YAG laser (50 mJ/pulse), a 1024x1008 pixels camera (model 630046, PIV CAM 10-30), and a Pentium P4 processor desktop. PIV seeding was provided by an American DJ smoke generator. To capture and process the PIV data, the INSIGHT (version 2.5) software was used.

Plasma Actuators

Plasma actuators used for these experiments were prepared by using copper as the material for electrodes and Alumina ceramic and Kapton as the materials for the dielectric. A copper tape was used for the exposed electrode of size 76.2 mm x 25.4 mm x 0.0254 mm and a rectangular piece from a copper sheet was used for the bottom electrode of the size 76.2 mm x 25.4 mm x 0.508 mm. The size of the Alumina ceramic material was 114.3 mm x 114.3 mm x 0.635 mm and the Kapton material size was 114.3 mm x 114.3 mm x 0.254 mm. The actuator was placed on a Plexiglas base with a size of 114.3 mm x 139 mm. The actuator's basic construction along with its dimensions is shown in Figure 3.2 (a) and a sample Kapton dielectric-based actuator is shown in Figure 3.2 (b). The actuator was placed in the closed enclosure (box) made of Plexiglas of size 1 m x 1 m x 1.5 m and the

box had a smoke passage that connected to the smoke generator. This box is capable of holding the smoke for at least two minutes.

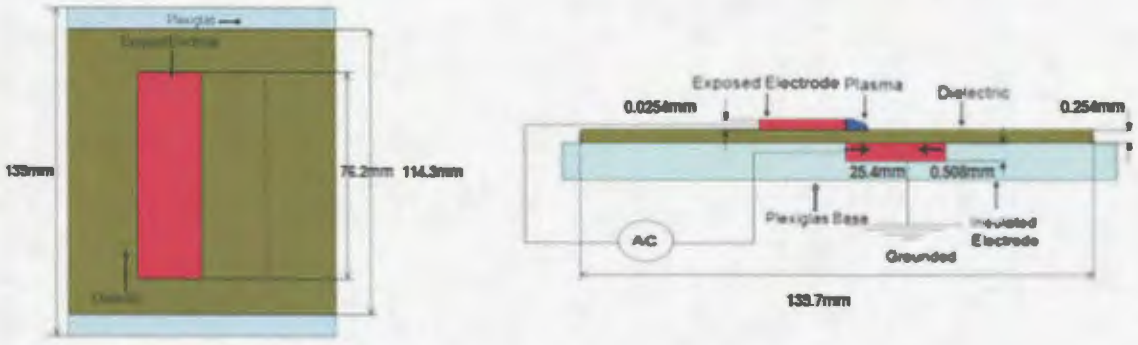

(a). Schematic & dimensions

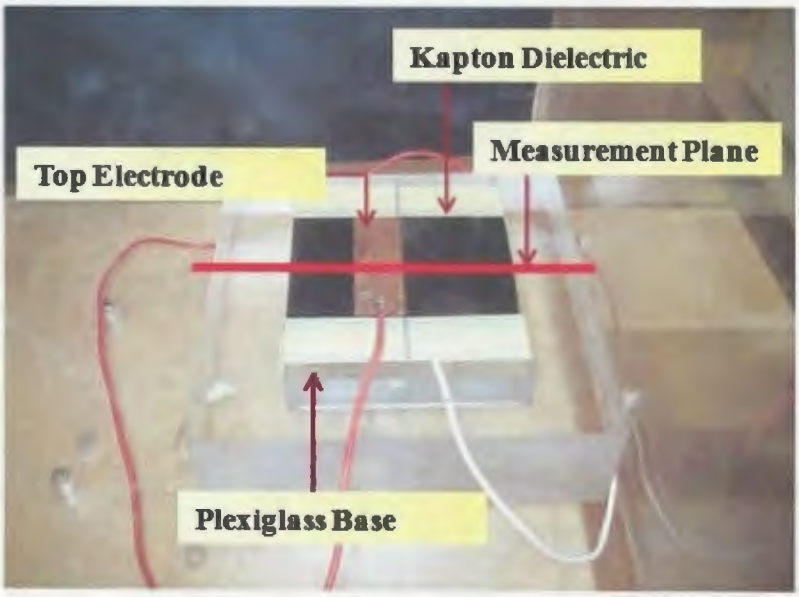

(b). Kapton actuator

Figure 3.1. Single dielectric barrier discharge actuator.

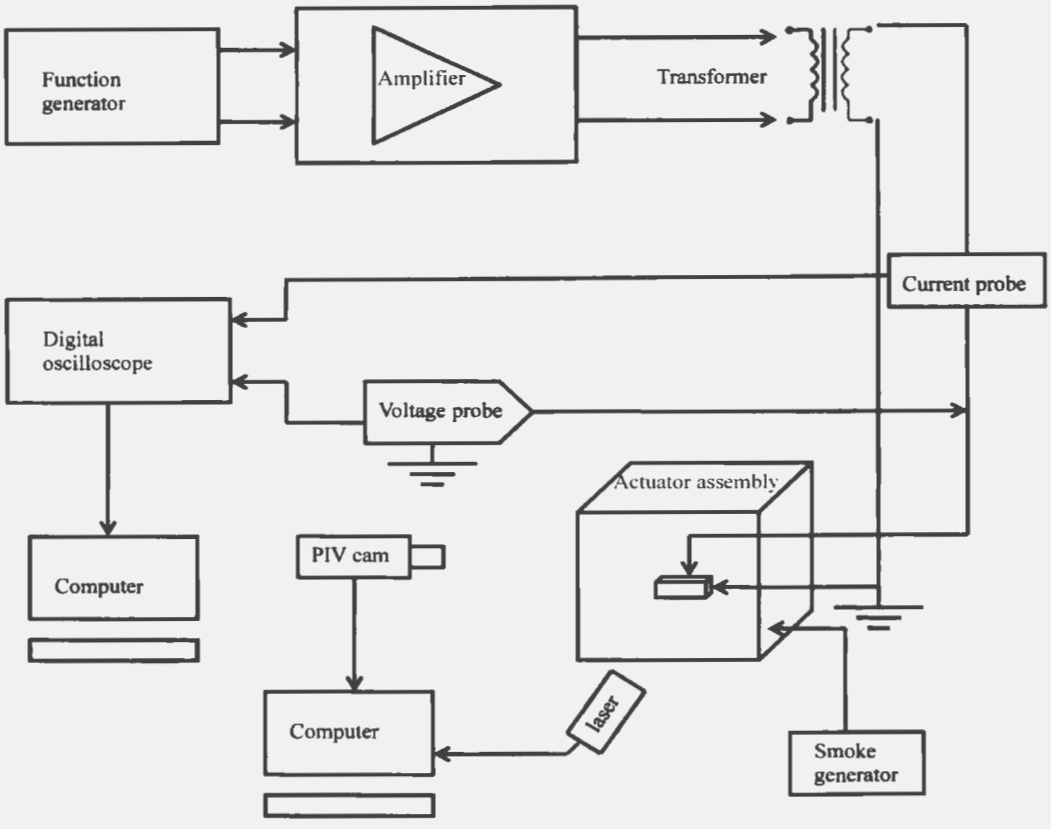

a) Schematic

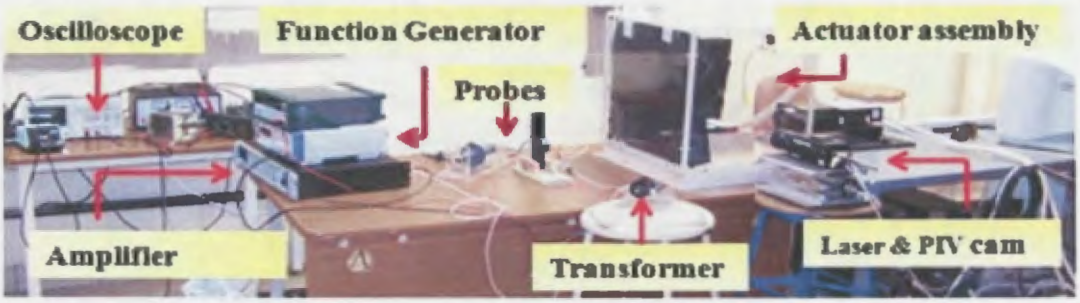

b) Experimental set-up

Figure 3.2. Schematic and experimental set-up.

The schematic (see Figure 3.2 (a)) shows that the A.C. power signal from the power source (function generator, amplifier and transformer) was supplied to the actuator which

was placed in the box. With the help of a PIV measuring system (laser, PIV cam), the PIV image data was captured and transferred to the computer, and the PIV seeding was performed using the smoke generator. The voltage and current measurements were performed by connecting the voltage probe with a parallel connection and the current probe with a series connection to the transformer output. The obtained voltage and current data were transferred to the computer with the help of a digital oscilloscope. To supplement a schematic diagram, a photograph of the experimental set-up is shown in Figure 3.2 (b).

3.2. Experimental arrangements

In the single DBD plasma actuator used for these experiments, the bottom electrode was buried or encapsulated in Plexiglas to avoid the plasma flow on the bottom side and it was glued into the slot created. One more slot was created on the Plexiglas for the cable access for the bottom electrode. The dielectric material (Alumina ceramic or Kapton) sheet was glued on the top of the bottom electrode, and copper tape (in the same area as the bottom electrode with different thickness) was pasted on top of the dielectric material. Overall, electrodes and dielectric materials are sandwiched together, which is how actuators are constructed.

Experiments were supposed to be performed in the quiescent media under ambient pressure and temperature conditions, so the actuator used was placed in the box and not tightly sealed. Once the PIV seeding was introduced into the box, the smoke particles were not clearly visible in the computer as the number of smoke particles increased. Some of the smoke particles were removed to avoid high density, and the time allowed for the smoke to settle down normally varied from about 1 to 1.5 minutes before the data were collected.

The laser used for these experiments consists of two lenses, a cylindrical and a bi-convex lens. The cylindrical lens is used to create a 2D sheet, and the bi-convex lens used to focus the laser placed on the actuator centerline has a focal length of 101.6 mm; therefore, the laser was attached to the box for better illumination. PIV measurements were taken by placing the camera on a stool with the box and laser placed on two different tables. The camera and the laser were arranged perpendicular to each other, as shown in Figure 3.3.

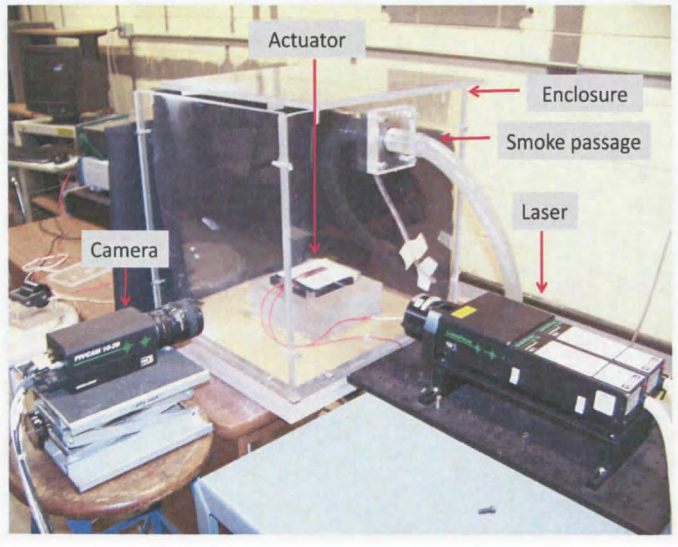

Figure 3.3. The PIV measurement system set-up.

The PIV calibration was done by placing a ruler on the center of the actuator (location of the laser plane) and recording the ruler images. Using the recorded ruler images, the pixels were converted into millimeters. To avoid the reflection from the glass, the inner wall of the box was covered with a black sheet. A set of data was taken at different time steps (dt), to obtain appropriate displacement of the particles in between the two frames of the PIV data. The time steps were chosen so that the maximum pixel displacement was in between one-third and one-fourth of the chosen interrogation window

(spot size). The primary correlation window (spot size) chosen was 32 pixels, and the Gaussian two-frame cross-correlation method was used to estimate the velocity between the two frames. To set the number of images required for the average velocity mapping accuracy, a study was performed by computing the average velocity distribution using different sets of images (sets of 450, 200 and 50 images). The optimum number of images required was chosen as 200 because any increase in the number of images beyond 200 did not change the average velocity profile. From the average maximum velocity of these three sets, there was no change in the maximum velocity from 200 images to 450 images, but there was a change of around 10% when compared to the 50 images.

3.2.1. PIV measurements

The voltage signal was supplied by turning on the function generator along with the amplifier and transformer. The PIV images were captured by using the INSIGHT software while the actuator was running. For each run 250 images were collected. Out of the 250 double-frame images, 200 images were averaged, as the first 30 to 50 images represented the developing stage of the plasma. All double-frame data with frames A and B corresponded with the first and second pulses of the laser; the laser pulses were sequenced by the synchronizer at the desired time steps (dt). A vector file for each data set was created, using the Gaussian two-frame cross-correlation method. The vector files represented a portion of the whole image, which depended on the location of the plasma actuator, and this portion was set by a specific interrogation area. This selected interrogation area was around 80 mm x 22 mm. Interactive validation filters were used to remove bad vectors from the vector files. The filters considered for these experiments were

range and mean. The range was fixed to clear the bad vectors, and the mean filter was used to fill the holes. This particular vector file with no bad vectors was read onto a macro file. The batch processing on all other vector files was done using this macro file. After vector post-processing using the validation filters, the average vector file was created, and it was also created in the form of a TECPLOT layout file. The maximum velocity area was determined from these TECPLOT vector contours. The same procedure was repeated for the rest of the experiments.

3.2.2. Data acquisition

To obtain the power data, the supplied voltage signal and current signal to the actuator were fed onto the computer with the help of the LABVIEW program, and these data were taken along with the PIV data. The data from these probes were supposed to be read directly into a computer using NIDAQ through BNC connectors attached to the probes; however, due to the impedance mismatch, the voltage readings were inaccurate. Therefore, a digital oscilloscope was used to read these data from the probes. The oscilloscope data read were then streamed onto a computer using a LABVIEW VI (virtual interface) provided by the oscilloscope manufacturer. The LABVIEW VI was modified based on our requirements, which included the addition of data storage VI to the original VI provided by the oscilloscope manufacturer. This modification helped in storing the data in the spreadsheets.

CHAPTER 4. RESULTS AND DISCUSSION

The laboratory experiments were designed to study the effect of the parameters such as voltage, frequency, electrode gap and dielectric material on the performance of the single dielectric barrier discharge (DBD) plasma actuators. These experiments were performed by varying one parameter at a time, keeping the other parameters constant (for example, the frequency was varied from 5 kHz to 15 kHz while keeping the voltage, electrode gap, and the dielectric material constant).

The parametric studies were conducted for different dielectric materials (Alumina and Kapton) with different electrode gaps (overlap, no gap, and 1 mm gap), and these dielectric materials with different gaps were operated at different voltages and frequencies. The operating conditions for different dielectric materials with each gap are tabulated in Table 4.1 below.

Table 4.1. Operating conditions

Material	Electrode Gap	Voltage range (kV)	Frequency range (kHz)
Al_2O_3(A)	1 mm overlap	2.8 – 4.2	5 -15
Al_2O_3(A)	No gap	2.8 – 4.6	5 -15
Al_2O_3(A)	1 mm gap	3.2 – 4.6	5 -15
Kapton(K)	1 mm overlap	2.8 – 4.2	5 -15
Kapton(K)	No gap	2.8 – 4.2	5 -15
Kapton(K)	1 mm gap	2.8 – 4.2	5 -15

All the materials with different electrode gaps were operated at a voltage range of 2.8 kV to 4.2 kV. The voltage variation was performed in two steps (from 2.8 kV to 3.5 kV and from 3.5 kV to 4.2 kV). Alumina dielectric material with no gap and 1 mm gap were

tested at a voltage of 4.6 kV, as they were able to operate at that particular high voltage. The lowest voltage of 3.2 kV was considered for Alumina with 1 mm gap as it showed inconsistent data at 2.8 kV. Both materials with different electrode gaps were tested for eight different operating frequencies ranging from 5 kHz to 15 kHz, with 1 kHz increments up to 10 kHz and discrete frequencies of 12 kHz and 15 kHz closed.

The typical voltage and current signals as measured from the plasma actuator at a constant frequency of 7 kHz are shown in Figure 4.1.

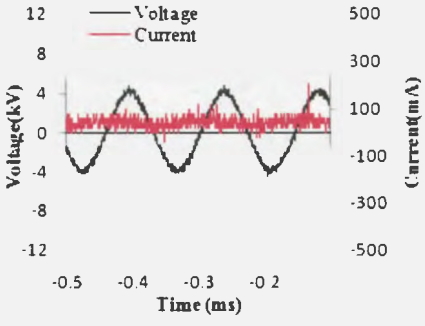

Figure 4.1. The current and voltage plots at a frequency of 7 kHz and voltage of 2.8 kV.

The performance of the single DBD plasma actuator was estimated based on the produced maximum velocity that was induced by the actuator on to the flow field. If the maximum velocity increases for the actuator by changing one parameter then we can say that the actuator showed higher performance with a change in that particular parameter. The performance of the single DBD plasma actuator was studied by analyzing the PIV images. The raw PIV images were processed using the INSIGHT software to obtain the vector data file, which was then exported to the TECPLOT software to obtain the velocity contours. Figure 4.2 shows a raw PIV image (single frame), the velocity vector (obtained

from the INSIGHT software) and the velocity contour plots (created in TECPLOT). The flow direction in all the images was from left to right. The location of the electrodes and the maximum velocity region are shown in the contour plot. The velocities referred to in the subsequent discussions are taken from the maximum velocity region (shown in Figure 4.2 (c)).

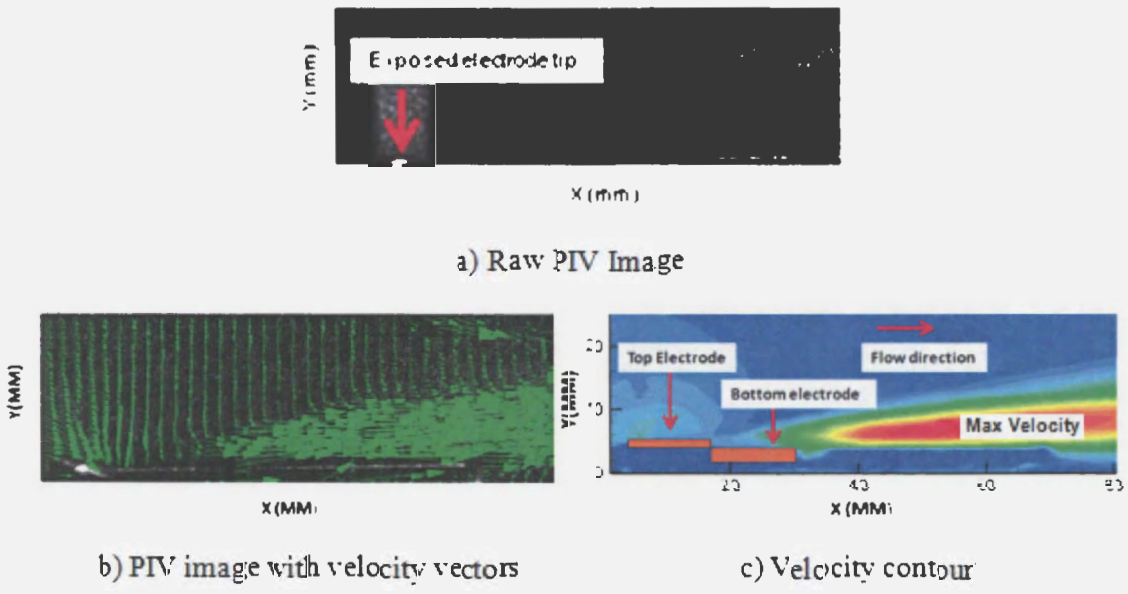

a) Raw PIV Image

b) PIV image with velocity vectors

c) Velocity contour

Figure 4.2. Velocity data plots.

The voltage and frequency effects on the plasma actuator's performance are discussed together in section 4.1 as their effects are closely related to each other. The results of the effects of the other parameters, such as dielectric material and electrode gap, are discussed in sections 4.2 and 4.3, respectively.

4.1. Voltage and frequency

The variation of the plasma-induced velocities with varying voltage and frequency is discussed in this section for both dielectric materials with different electrode gaps. The results of the velocity changes with changing voltage and frequency are plotted together in Figure 4.3 for different electrode gaps and dielectric materials. Figure 4.3 illustrates that the operating voltage and frequency influence the overall performance of the DBD plasma actuators. Previous studies have stated that an increase in voltage increases the plasma-induced velocity due to an increase in the electric field, which results in more Colombian forces between ions, and which pushes the surrounding medium with a higher velocity or momentum. The increase in frequency also increases the plasma-induced velocity because it speeds up the rate of collisions between ions and electrons, and that results in the plasma pushing the surrounding medium with higher velocity[11]. A similar observation was noted in the present study with voltage and frequency increases.

The data collected for this research were processed after the experiments were completed. Although the data were verified randomly after collection, some data were found to be too inconsistent and unreliable to present in this discussion. These data sets could not be repeated later; therefore, the data for some frequencies are not presented. The obtained data showed consistency up to 9 kHz frequency. The variation of the induced velocities was found to be almost linear except for Alumina with 1 mm overlap and 1 mm gap with increasing voltages. The effect of the frequency on the plasma-induced velocity was less significant for the constant voltage of 2.8 kV, but it was dominant at intermediate voltages (see Figure 4.3).

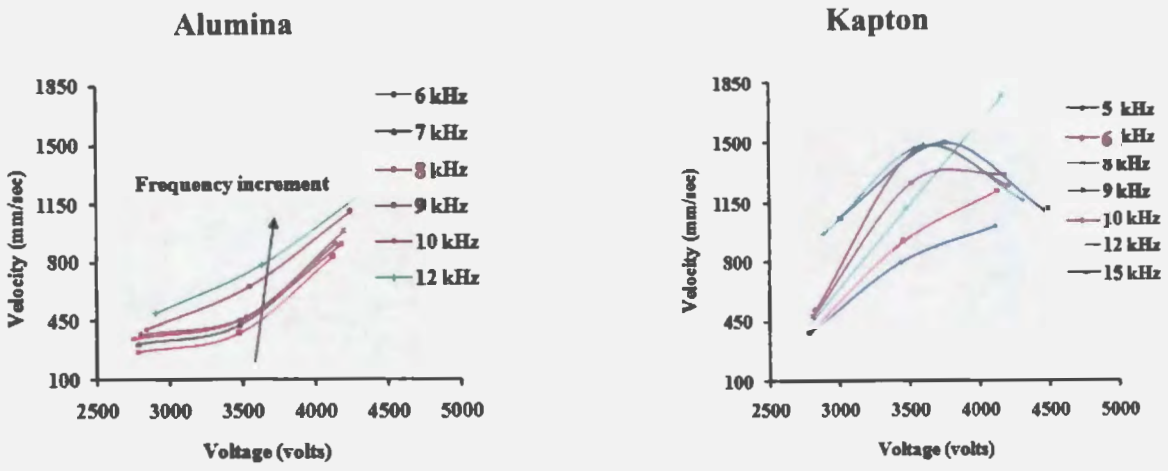

a) 1 mm overlap

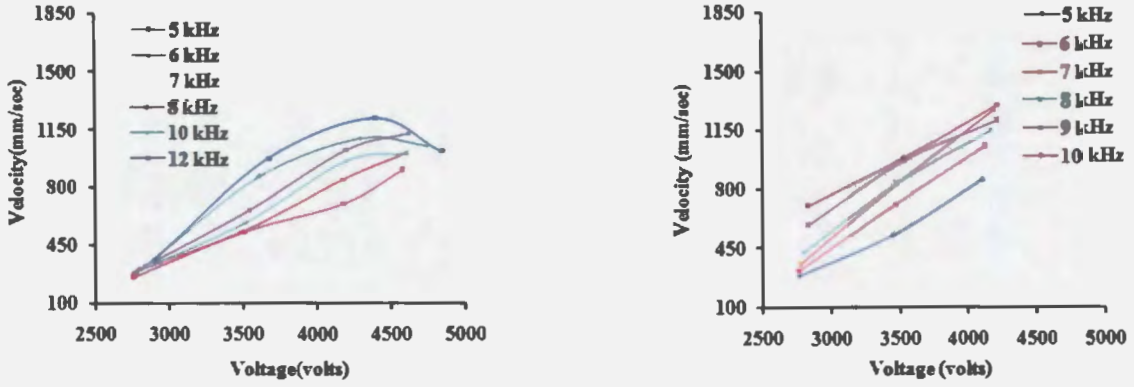

b) No gap

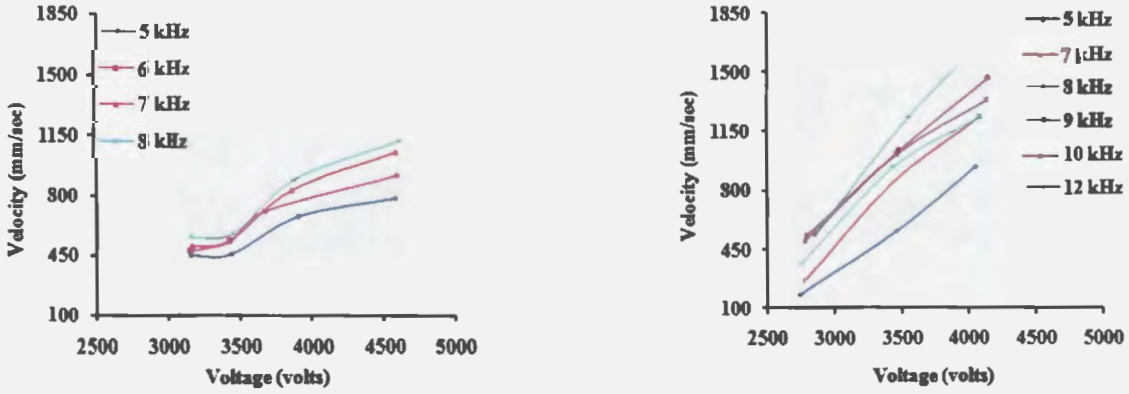

c) 1 mm gap

Figure 4.3. Velocity vs. voltage at different frequencies for different electrode gaps and dielectric materials.

At higher frequencies (more than 9 kHz), Kapton with 1 mm overlap at 4.2 kV and Alumina with no gap at 4.6 kV showed low velocities when compared to the velocities at intermediate voltages. This was due to filamentary instabilities[11,12].

The voltage effect on the plasma-induced velocity was more when compared to the frequency effect. To further analyze the voltage and frequency effects in a quantitative manner, the Alumina with 1 mm overlap was considered and the data for 6 kHz and 12 kHz are presented in Table 4.2. The velocity increase at a lower voltage step (6 kHz) was about one-third of the velocity increase at a higher voltage step. However, at the constant frequency of 12 kHz, the plasma velocity increase was observed to be about 60% in both voltage steps.

Table 4.2. The maximum induced velocity at different voltages for 1 mm overlap

Plasma Voltage (kV)	Voltage range (kV)	Frequency range (kHz)
2.8	269	500
3.5	375	790
4.2	833	1240

A clear distinction can be made from the Alumina and Kapton data. The data are more consistent with Kapton for a wider range of frequencies and the overall induced velocities produced are higher at varying voltages and frequencies. Kapton showed linear variation in the velocity vs. voltage curves at constant frequencies (see Figure 4.3). The effect of frequency varied with varying dielectric materials from Alumina to Kapton (see Figure 4.3). Variation in the electrode gap has not shown significant impact on the voltage

and frequency effects on the velocity, especially for Alumina dielectric material. Overall, the plasma actuator performed better with Kapton dielectric materials.

For a better qualitative comparison on the voltage effect on the Alumina with an electrode gap of 1 mm overlap, the velocity contour plots at each operating voltage are shown in Figure 4.4.

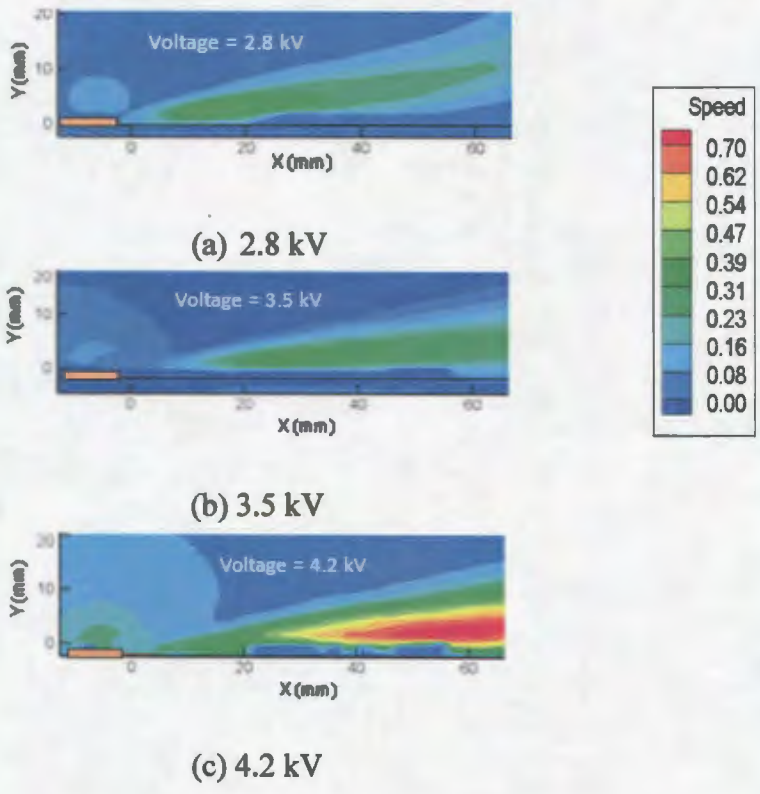

Figure 4.4. Velocity distribution at different voltages for a constant frequency of 6 kHz for Alumina with 1 mm overlap between electrodes.

The induced flow starts out horizontally near the tip of the electrode and then expands at an angle downstream. At higher voltages, the maximum velocity area shifts further downstream.

The profiles were taken at constant frequency (6 kHz) and at varying voltages. Figure 4.5 shows that the maximum velocity region is shifted downstream at higher voltages and the area of the maximum velocity region is enlarged at higher voltages giving more momentum to the flow.

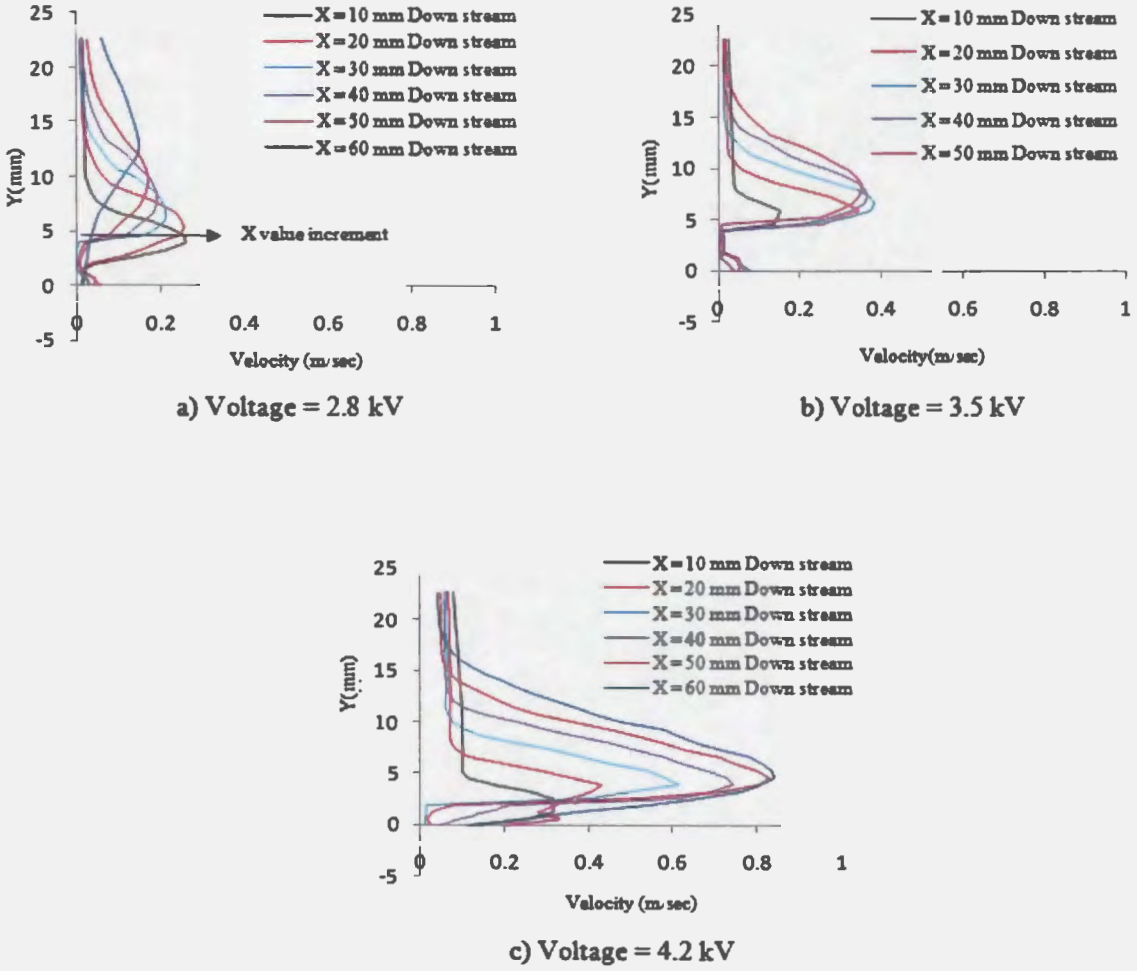

a) Voltage = 2.8 kV

b) Voltage = 3.5 kV

c) Voltage = 4.2 kV

Figure 4.5. Downstream velocity profiles for different voltages at constant frequency of 6 kHz for Alumina with 1mm overlap between electrodes.

The influence of the operating frequency on the plasma performance was also shown in Figure 4.3. The data showed minimal effect on the plasma-induced velocity with increasing frequency at the lowest constant voltages, although the velocity increase was

higher at higher frequencies. Unlike voltage effects, the velocity variation was observed linearly for the range of frequencies studied. Figure 4.6 shows velocity variation with increasing frequencies for a constant voltage of 2.8 kV for Alumina with an electrode gap of 1 mm overlap. This linear variation with identical slopes (parallel) can also be observed at the other voltages (up to 4.2 kV).

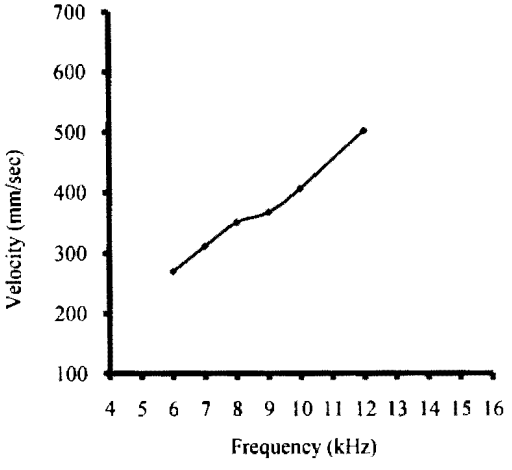

Figure 4.6. Velocity vs. frequency plot at 2.8 kV for 1 mm overlap between electrodes.

For a better understanding, Figure 4.7 shows the velocity contour plots at 6 and 12 kHz frequencies at a constant voltage (2.8 kV). The increased velocity at a higher frequency can be seen in the figure, although the velocity jump in the core was only about two-thirds as the frequency was doubled. Referring back to Table 4.2, the frequency effect (6 to 12 kHz) on the increase in velocities can be seen where doubling the frequency provided only up to a 60% increase in velocities.

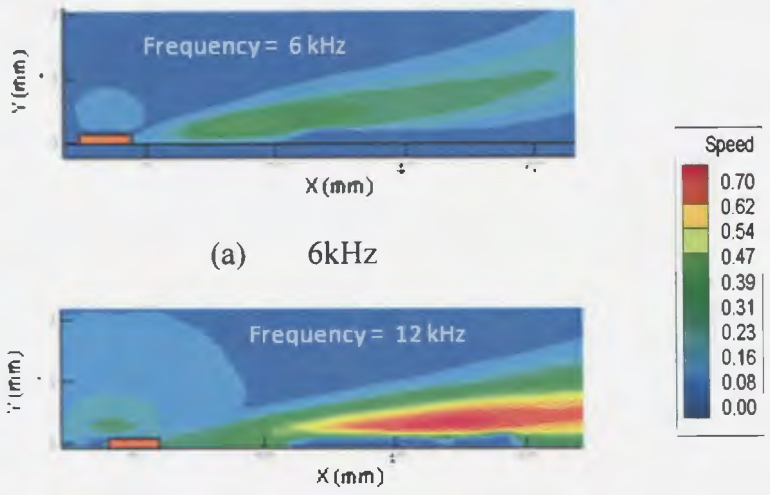

(a) 6kHz

(b) 12 kHz

Figure 4.7. The velocity contour plots at 6 and 12 kHz frequencies at constant voltage for 1 mm overlap between electrodes.

4.2. Electrode gap

In addition to the above-mentioned parameters, one more important parameter to discuss is the electrode gap. The data with frequencies up to 9 kHz were considered to explain this effect. The velocity and power vs. frequency for electrode gap plots were used to explain the effect of the electrode gap (1 mm overlap, no gap and 1 mm gap) on the plasma-induced velocity, and they were plotted for the constant voltage of 2.8 kV.

Alumina dielectric material with different electrode gaps was plotted in Figure 4.8, and from the figure it is clear that the velocity produced was high for the 1 mm gap case with less power consumption. Previous studies have stated that increasing the gap increased the plasma expansion length which resulted in higher induced velocity, and the same observation was noticed here[11,12]. Figure 4.9 was plotted for Kapton material cases. The 1 mm overlap showed the highest velocities whereas the 1 mm gap showed the lowest velocities. Figure 4.9 (b) illustrates that the power consumption value for all the gaps is

almost equal. Unlike the Alumina material results, the 1 mm overlap case has shown higher velocities. This observation is different from previous observations[11,12,15].

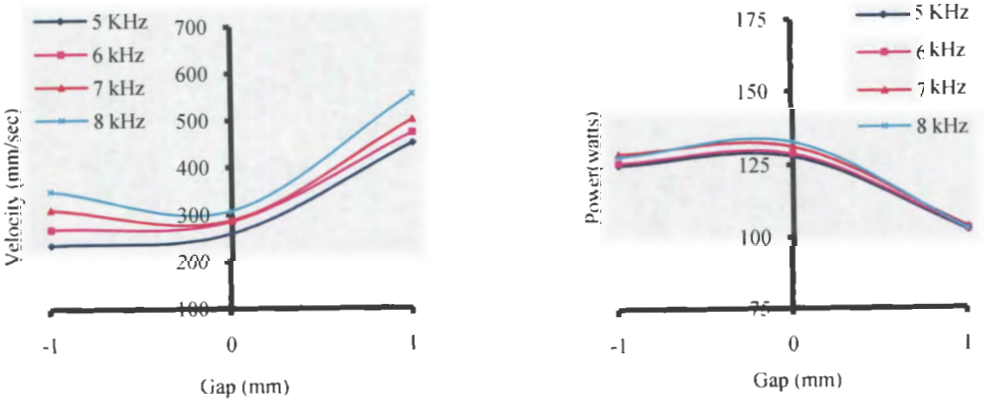

(a) Velocity vs. electrode gaps (b) Power vs. electrode gaps

Figure 4.8. Velocity and power vs. electrode gaps at different frequencies.

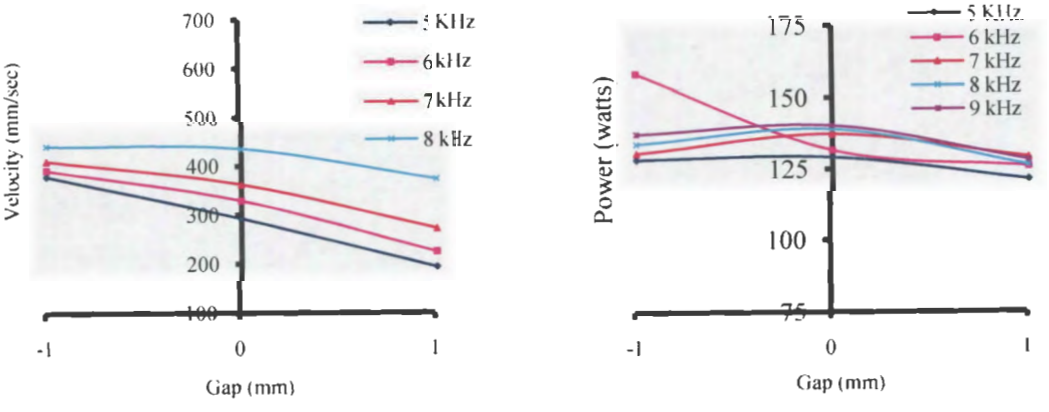

(a) Velocity vs. electrode gaps (b) Power vs. electrode gaps

Figure 4.9. Velocity and power vs. electrode gaps at different frequencies.

Finally, the electrode gap has not shown considerable impact on the plasma-induced velocity and most of the data showed randomness in the results. These changes might be due to experimental uncertainties.

4.3. Material

In the material parameter, the permittivity and dielectric strength played key roles, and the dielectric materials considered were Kapton and Alumina ceramic. Kapton has a higher dielectric strength (154 kV/mm) and lower permittivity ($\varepsilon_r = 3.5$), whereas Alumina ceramic has a lower dielectric strength (15 kV/mm) with higher permittivity ($\varepsilon_r = 9.4$). At lower voltages, high permittivity induces higher velocity, but at higher voltages (less than 4 kV), the velocity decreases as the dielectric loss factor increases along with the voltage[11]. The dielectric strength helps it to sustain the actuator at higher voltages and frequencies. In order to find the effect of the dielectric material impact on the DBD plasma actuator, the data were arranged based on the materials at the voltage of 2.8 kV. In order to evaluate the effect of the material on the single DBD plasma actuator, velocity and power vs. frequency was plotted and compared for 1 mm overlap and no gap. One important thing to mention is that Alumina is 2.5 times thicker than Kapton.

Figure 4.10 (a) illustrates that Kapton performed better than Alumina with more velocities as the frequency increased from 5 kHz to 9 kHz. Even though the Kapton has low permittivity, compared at a lower voltage such as 2.8 kV, it still produced higher velocities. The Kapton is thinner than Alumina, and the thinner material produces a higher velocity as the permittivity of the material depends on the thickness of the material. Figure

4.10 (b) shows that the power consumption is slightly higher for Kapton materials except at 6 kHz. A similar observation is found in Figure 4.11.

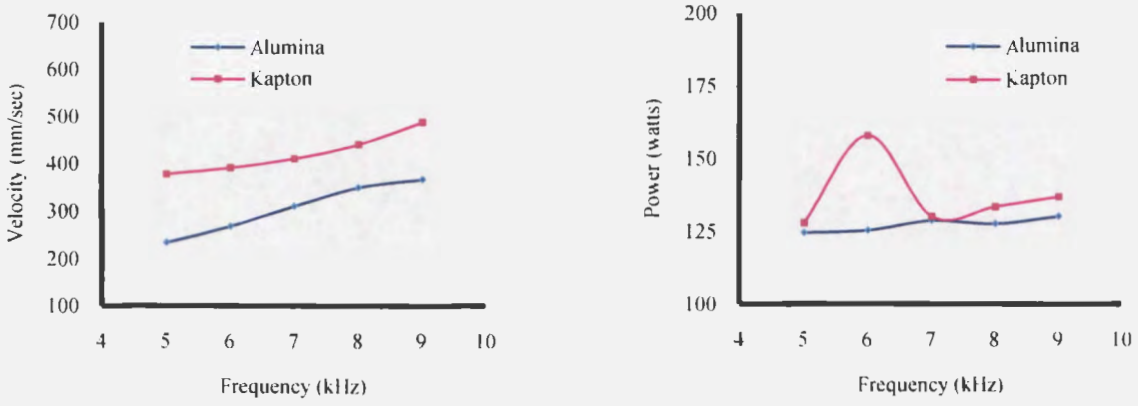

(a) Velocity vs. frequency (b) Power vs. frequency

Figure 4.10. Velocity and power vs. frequency for the Alumina and Kapton materials at 1 mm overlap gap.

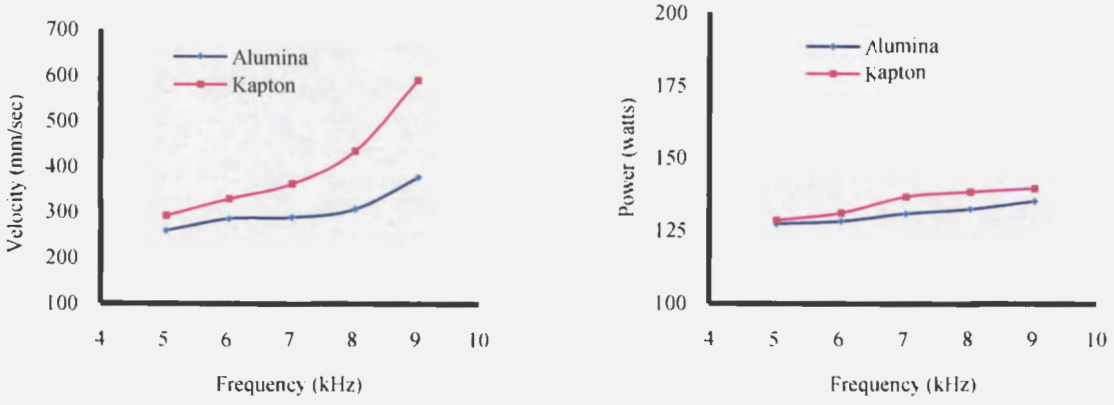

(a) Velocity vs. frequency (b) Power vs. frequency

Figure 4.11. Velocity and power vs. frequency for the Alumina and Kapton materials at no gap.

Overall, by comparing all the cases, the material effect on the plasma-induced velocity is less significant, but the Kapton dielectric material produced higher velocities irrespective of thickness, except in the 1 mm gap case.

CHAPTER 5. CONCLUSIONS

A parametric study to characterize a single dielectric barrier discharge (SDBD) plasma actuator was conducted with 1) voltage, 2) frequency, 3) electrode gap, and 4) dielectric materials as primary parameters. This parametric study has provided an opportunity to understand the plasma behavior at lower voltages (less than 4 kV) and at higher frequencies (greater than 5 kHz) with small electrode gaps (±1 mm) and two dielectric materials (Alumina, Kapton). The performance of the SDBD plasma actuator was determined by the plasma-induced velocity, measured using a PIV system in quiescent media.

The first parameter (voltage) was observed to have a major influence on the induced velocity. The voltage studied was 2.8 to 4.6 kV. The data revealed that a higher voltage induced a higher velocity. However, the operating voltage is related to the operating frequency (the second parameter); therefore, the increase in velocity with voltages was observed for frequencies up to 9 kHz. The velocity was observed to have peak value at an intermediate voltage at higher frequencies (greater than 9 kHz). The second parameter (frequency) was observed to have a small effect on the plasma velocity for Alumina dielectric but showed significant effect for the Kapton dielectric. To observe a comparable effect in the induced velocity for Alumina, the relative increase in frequency needed is more than 100%; for example, a 100% increase in frequency led to a 30 to 80% increase in velocity, whereas the same velocity increase could be achieved at a 20 to 25% increase in voltages. The Kapton with different gaps frequency showed almost the same effect as the voltage and 100% increase in frequency led to an 80 to 100% increase in the velocity. The frequency effect on the velocity becomes dominant at higher operating

voltages. Overall, the induced velocities increased linearly with increasing frequencies but at a lower rate at higher frequencies.

The effect of the third parameter (electrode gaps) was studied within the small range of electrode gaps (±1 mm gap). The data analysis revealed that the fluctuations in the velocity (increase or decrease) due to electrode gap orientations were mainly due to experimental uncertainties. The overall influence of the electrode gap orientations within a 1 mm range showed no impact on the plasma-induced velocities with random data.

Finally, the effect of the fourth parameter (materials), using Alumina and Kapton, was studied to determine the effects in plasma performance. The overall effect of the materials was negligible in producing plasma-induced velocities. However, comparing the relative performances, Kapton produced higher velocities at the same operating conditions.

BIBLIOGRAPHY

1. M. Samimy, I. Adamovich, J.-H. Kim, B. Webb, S. Keshav, and Y. Utkin "Active Control of High Speed Jets Using Localized Arc Filament Plasma Actuators" AIAA 2004-2130; 2nd AIAA Flow Control Conference, 28 June - 1 July 2004, Portland, Oregon.

2. M. Samimy, I. Adamovich, B. Webb, J. Kastner, J. Hileman, S. Keshav, P. Palm "Development and characterization of plasma actuators for high-speed jet control" Experiments in Fluids 37 (2004) 577–588.

3. M. Samimy, J.-H. Kim, J. Kastner, I. Adamovich, and Y. Utkin "Active Control of High-speed and High Reynolds Number Jets Using Plasma Actuators" J. Fluid Mech. (2007), vol. 578, pp. 305–330.

4. N. Benard J. Jolibois M. Forte G. Touchard, E. Moreau "Control of an axisymmetric subsonic air jet by plasma actuator" Exp Fluids (2007) 43:603–616, DOI 10.1007/s00348-007-0344-9.

5. Arvind Santhanakrishnan , Jamey D. Jacob and Y. B. Suzen "Flow Control Using Plasma Actuators and Linear/Annular Plasma Synthetic Jet Actuators" AIAA 2006-3033, 3rd AIAA Flow Control Conference, 5 - 8 June 2006, San Francisco, California.

6. Arvind Santhanakrishnan, and Jamey D. Jacob "On Plasma Synthetic Jet Actuators" 44th AIAA Aerospace Sciences Meeting and Exhibit, Jan. 9–12, 2006, Reno, NV.

7. Arvind Santhanakrishnan and Jamey D Jacob "Flow control with plasma synthetic jet actuators" Journal of Physics D: Applied Physics, J. Phys. D: Appl. Phys. 40 (2007) 637–651.

8. C. L. Enloe, Thomas E. McLaughlin, Robert D. VanDyken, K. D. Kachner , Eric J. Jumper and Thomas C. Corke "Mechanism and responses of a single dielectric barrier plasma actuator"AIAA 2003-1021, 41st Aerospace Sciences Meeting and Exhibit, 6-9 January 2003, Reno, Nevada.

9. C. L. Enloe, Thomas E. McLaughlin, Robert D. VanDyken, K. D. Kachner , Eric J. Jumper and Thomas C. Corke "Mechanism and responses of a single dielectric barrier plasma actuator: Plasma Morphology" AIAA Journal Vol. 42, No. 3,pages : 590-596, March 2004.

10. C. L. Enloe, Thomas E. McLaughlin, Robert D. VanDyken, K. D. Kachner , Eric J. Jumper, Thomas C. Corke, M.post and J.Haddad "Mechanism and responses of a single dielectric barrier plasma actuator :Geometry effects" AIAA Journal Vol. 42, No. 3, pages : 596-604, March 2004.

11. M. Forte, J. Jolibois J. Pons, E. Moreau, G. Touchard and M. Cazalens "Optimization of a dielectric barrier discharge actuator by stationary and non-Stationary measurements of the induced flow velocity: application to airflow Control" Exp fluids (2007) 43 : 917-928.

12. J. Reece Roth and Xin Dai "Optimization of the Aerodynamic Plasma Actuator as an Electro Hydrodynamic (EHD) Electrical Device" 44th AIAA aerospace Science meeting and exhibit; 9-12 January 2006, Reno , Nevada.

13. Takashi Abe, Yuji Takizawa, and Syunichi Sato and Nobara Kimura "A Parametric Experimental Study for Momentum Transfer by Plasma Actuator" AIAA 2006-167, 45th AIAA Aerospace Meeting and Exhibit, 9-12 January 2006, Reno, Nevada.

14. Robert Van Dyken, Thomas E. McLaughlin and C. Lon Enloe "Parametric investigations of a single dielectric barrier discharge plasma actuator" 42nd AiAA Aerospace Sciences Meeting and Exhibit, 5-8 January 2004, Reno, Nevada.

15. J´er^ome Pons1, Eric Moreau and G´erard Touchard "Asymmetric surface dielectric barrier discharge in air at atmospheric pressure: electrical properties and induced airflow characteristics" Journal of Physics D: Applied Physics, J. Phys. D: Appl. Phys. 38 (2005) 3635–3642.

16. N.Balcon, N.Benard, Y.Lagmich, J-P. Boeuf, G. Touchard, E.Moreau "Positive and Negative saw tooth signals applied to a DBD plasma actuator -influence on the electric field wind" Journal of electrostatics 67 (2009) 140-145.

17. Brad A. Gibson , Maziar Arjomandi and Richard M.Kelso " Investigation of the Effect of Electrode Arrangement on Plasma Actuator Performance" AIAA 2009-1003 , 47th AIAA Aerospace Sciences Meeting Including The New Horizons Forums and Aerospace Explosion; 5-8 January 2009, Orlando , Florida.

18. Jamey D. Jacob and Karthik Ramkumar , Rich Anthony and Richard B. Rivir " Control of laminar and turbulent shear flows using plasma actuators " 4th International Symposium on Turbulence and Shear Flow Phenomena, Williamsburg, VA June 27–29, 2005.

19. Karthik Ramakumar and Jamey D. Jacob "Flow Control and Lift Enhancement Using Plasma Actuators" 35th Fluid Dynamics Conference, June 6-9, 2005, Toronto, ON.

20. Y. B. Suzen and P. G. Huang "Simulations of Flow Separation Control using Plasma Actuators" AIAA 2006-877, 44th AIAA Aerospace Sciences Meeting and Exhibit, 9 - 12 January 2006, Reno, Nevada.

21. Dmitriy M. Orlov , Thomas Apker, Chuan He, Hesham Othman and Thomas C. Corke "Modeling and Experiment of Leading Edge Separation Control Using SDBD Plasma Actuators" AIAA -2007-0877 AIAA 45th Aerospace Sciences Meeting, 8-11 January 2007, Reno, Nevada.

22. Y. B. Suzen, P. G. Huang, Jamey D. Jacob and D.E Aships " Numerical simulation of plasma flow control applications" AIAA 2005-4633, 35th Fluid Dynamics Conference and Exhibit, June 6-9, 2005, Toronto, Ontario.